Electron scattering from ^{88}Sr and ^{89}Y

S. P. Fivozinsky
National Bureau of Standards, Washington, D.C. 20234
Physics Department, The University of Connecticut, Storrs, Connecticut 06268

S. Penner and J. W. Lightbody, Jr.
National Bureau of Standards, Washington, D.C. 20234

D. Blum
Laboratoire de l'Accelerateur Lineaire, Orsay, France
(Received 26 November 1973)

Inelastic scattering cross sections of low-lying levels and elastic scattering cross sections have been measured in ^{88}Sr and ^{89}Y using the National Bureau of Standards Linac and electron scattering facility. Incident-electron energies were varied between 45 and 121 MeV corresponding to a momentum transfer range of 0.4 to 1.0 fm^{-1}. Data were accumulated at two scattering angles, 110.5 and 128.2°. We present elastic scattering form factors and inelastic scattering form factors and $B(EL)$↑'s for the 1.84- and 2.74-MeV states in ^{88}Sr, and the 1.51-, 1.74-, 2.21-, 2.52-, 2.86-, and 3.1-MeV states in ^{89}Y. A simple configuration mixing model based on the weak-coupling model has been applied to the octupole states in ^{89}Y. The measured elastic form factors for both nuclei have been fitted with a Fermi charge distribution.

[NUCLEAR REACTIONS ^{88}Sr(e,e'), ^{89}Y(e,e'), $E=45$–121 MeV, $\theta=110.5$, 128.2°; measured elastic, inelastic form factors, deduced $B(EL)$↑'s. Extracted charge distribution parameters. Predict $B(E3)$↑'s, form factors, ^{89}Y. Enriched ^{88}Sr target.]

INTRODUCTION

The suggestion that certain pairs of levels in ^{89}Y might be described by the weak coupling[1] of a $2p_{1/2}$ proton to the 2^+, 3^-, and 2^+ excited states of a ^{88}Sr core at 1.84, 2.74, and 3.2 MeV was made by Shafroth, Trehan, and Van Patter[2] as the result of an $(n,n'\gamma)$ experiment. Shafroth's scheme assigned the ^{89}Y pairs of states at 1.51 and 1.74 MeV, 2.21 and 2.52 MeV, and 2.86 and 3.1 MeV, respectively, to the ^{88}Sr core states mentioned above. Inelastic α[3] and proton[4] scattering experiments, however, showed that the state at 2.86 MeV in ^{89}Y had the opposite parity from that measured by Shafroth, resulting in a triplet of strong octupole transitions in ^{89}Y (Fig. 1). These results were in sharp disagreement with the weak-coupling scheme.

The single-particle nature of the states in ^{89}Y has also been investigated by the ^{88}Sr$(^3$He$,d)^{89}$Y reaction.[4,5] Proton stripping into the $2p_{1/2}$, $1g_{9/2}$, and $2d_{5/2}$ orbitals corresponds respectively to the ground state, 0.908-MeV isomer, and the 3.75-MeV state, indicating that the quadrupole and octupole transitions which lie between 0.908 and 3.75 MeV arise primarily from excitations of the core (Fig. 2).

Electron scattering measurements[6] on these nuclei at low momentum transfer (≤ 0.7 fm^{-1}) gave results which were consistent with the proton and α-particle inelastic scattering experiments. Also, electron scattering did not excite the 2^+ transition in ^{88}Sr at 3.2 MeV, but did strongly excite the 2.86-MeV level in ^{89}Y, emphasizing the independence of this level from the 3.2-MeV state in ^{88}Sr.

Proton pickup reaction experiments[7] $(d,{}^3$He$)$ on ^{90}Zr and ^{89}Y excited the 2^+ transitions in both ^{89}Y and ^{88}Sr, suggesting that these states have large single-hole components. On the other hand, none of the 3^- transitions in either nucleus were excited by this reaction, supporting their description as highly collective states.

A high-resolution proton inelastic scattering study[8] of the states in ^{89}Y has shown the state at 2.86 MeV probably to consist of two unresolved levels approximately 10 keV apart. The authors suggest that these two levels may be the negative-parity level seen by Shafroth and the positive-parity state seen in the inelastic scattering experiments, since the different experiments may preferentially excite one or the other level in this unresolved pair.

By means of electron scattering one can measure the behavior of the transition-matrix element of a given level as a function of momentum transfer. The momentum transfer (q) dependence can deter-

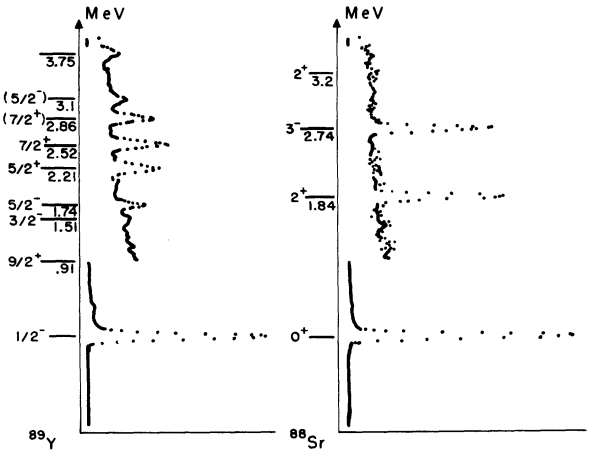

FIG. 1. Sample spectra of electrons scattered from ^{88}Sr and ^{89}Y and comparison to low-lying level diagrams.

mine multipole assignments as well as a choice of nuclear model to describe the transition. The differential scattering cross section for excitation of a level may be written in terms of the appropriate transition-matrix element, or equivalently in terms of a form factor

$$|F|^2 = \sigma_L/\sigma_M , \tag{1}$$

where σ_L is the differential cross section for exciting a transition of multipolarity L and σ_M is the Mott[9] cross section.

We have used the sensitivity of the form factor to the excited-state structure at higher momentum transfer by comparing q dependence of form factors having the same transition multipolarity to determine qualitatively whether a set of states in ^{89}Y displays the same excited-state structure as the core state in ^{88}Sr. In addition, all measured inelastic scattering form factors have been fitted with a distorted-wave Born-approximation calculation (DWBA) to determine reduced transition probabilities $[B(EL)\uparrow]$. A calculation of form factors and $B(E3)\uparrow$'s of the octupole triplet in ^{89}Y at 2.21, 2.52, and 2.86 MeV based on a mixed configuration model[10,11] has also been carried out.

In this experiment no separation of longitudinal and transverse contributions[12] to the cross section was attempted since the transverse part of an electric collective transition, for large Z, is expected to be very small[13,14] except at extreme forward or backward angles.

The elastic scattering form factors for both nuclei have been analyzed using the two-parameter Fermi charge density model given by

$$\rho(r) = \frac{\rho_0}{1+\exp[(r-c)/z]} , \tag{2}$$

where c is the half-density radius and $(4.4)z$ is the radial distance over which the density falls from 90 to 10% of its maximum value.

These measurements cover a momentum transfer region from 0.4 to 1.0 fm^{-1}, obtained by varying the incident energy between 45 and 121 MeV. The scattering angles used were 110.5 and 128.2°.

THEORY

A. Weak coupling

According to the ^{87}Sr$(d,p)^{88}$Sr reaction,[15] a neutron state does not appear until about 4 MeV excitation in ^{88}Sr. Thus, the low-lying levels in $N = 50$ nuclei should be describable primarily in terms of proton excitations. In ^{89}Y the ground state is given by a single proton in the $2p_{1/2}$ orbit coupled to the ^{88}Sr ground state (Fig. 2). The $\frac{9}{2}^+$ isomer at 0.908 MeV is constructed by promoting this proton to the $1g_{9/2}$ orbit. However, the next state, the $\frac{3}{2}^-$ at 1.51 MeV, is most easily constructed by promoting a proton from the filled $2p_{3/2}$ orbital in the core to pair with the $p_{1/2}$ pro-

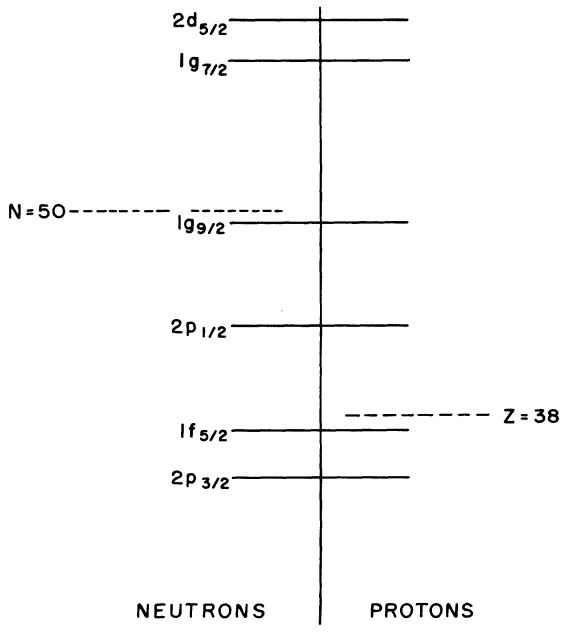

FIG. 2. Shell-model orbitals in the region of $N = 50$.

TABLE I. Parameters determined from fitting configuration mixing model to 3^- transitions in ^{89}Y.

α	β	Harmonic-oscillator parameter (fm)
0.9927 ± 0.0012	0.9593 ± 0.0018	2.254 ± 0.016

ton. A similar description holds for the $\frac{5}{2}^-$ state at 1.74 MeV in terms of the $1f_{5/2}$ orbital. (This suggests that the usual ordering of the $2p_{3/2}$ and $1f_{5/2}$ proton orbitals is reversed.) Both the $\frac{3}{2}^-$ and $\frac{5}{2}^-$ states are found to be populated strongly in the proton pickup reaction on ^{90}Zr.[7] If ^{88}Sr is mostly a closed core, the $\frac{3}{2}^-$ and $\frac{5}{2}^-$ states should be weakly populated in the proton stripping reaction on ^{88}Sr. Stripping spectroscopic factors[5] indicate that the $2p_{3/2}$ orbital has a fractional emptiness of about 10% and the $1f_{5/2}$ about 10%.

One may instead consider the weak-coupling model[1] which also properly predicts the spins and parities of the ^{89}Y levels at 1.51 and 1.74 MeV as the coupling of the $2p_{1/2}$ proton to the lowest 2^+ excitation in ^{88}Sr. In addition, this model lends itself more readily than a shell-model description to a discussion of the collective 3^- transitions occurring in ^{89}Y between 2 and 3 MeV.

The wave function for such a core excited state is written

$$|J_c j,\ JM\rangle,$$

where J_c is the core angular momentum, j is the angular momentum of the particle, and J is the total angular momentum, with $J_z = M$. The degeneracy of the $2j+1$ levels of the "core multiplet" based on core state J_c is removed by the particle-core interaction. The strengths of the members of a multiplet are given by

$$B_J(EL)\uparrow = \frac{2J+1}{(2j+1)(2J_c+1)}\, B_c(EL)\uparrow, \tag{3}$$

where $B_c(EL)\uparrow$ is the strength of the core state, so that the sum of the strengths of the multiplet equals the strength of the core state.

We naturally identify the core state in the odd-even nucleus with the corresponding state in the neighboring even-even nucleus. This is not necessarily a good identification since the presence of the odd nucleon in state j will partially block[16] the core excitation via the Pauli principle. The similarity to the corresponding state in the even-even nucleus should be proportional to the collectivity of that state since the presence of a single particle will have a very small effect on a highly collective excitation. One expects that if a state in the odd-even nucleus is a member of a weak-coupling multiplet, its electron scattering form factor will have the same momentum transfer (q) dependence as the collective excitation in the corresponding even-even nucleus. If we write the transition multipole operator Ω^L as a sum of core and particle parts,

$$\begin{aligned}\langle J_c' j,\ J_f \| \Omega_c^L + \Omega_p^L \| J_c j,\ J_i\rangle &= A\langle J_c' \| \Omega_c^L \| J_c\rangle + B\langle j \| \Omega_p^L \| j\rangle \\ &= A\langle J_c' \| \Omega_c^L \| J_c\rangle,\end{aligned} \tag{4}$$

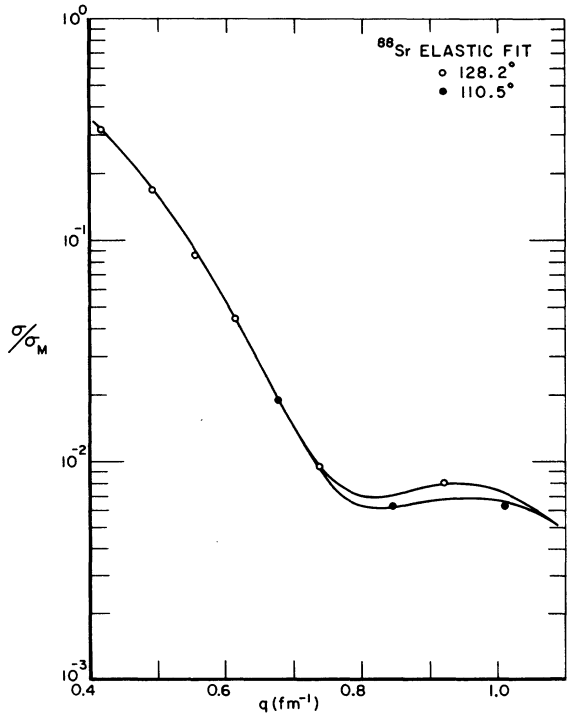

FIG. 3. Fermi-model fit to ^{88}Sr elastic form factor.

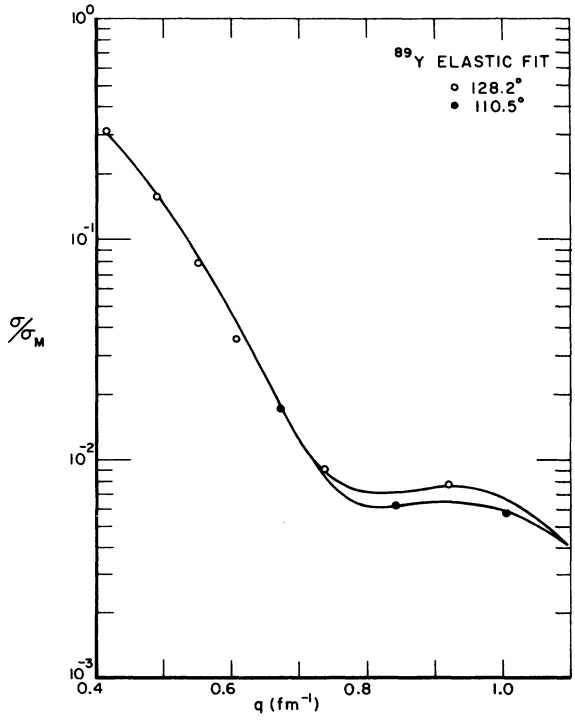

FIG. 4. Fermi-model fit to ^{89}Y elastic form factor.

since the particle undergoes no transition. A and B are statistical factors and L is the multipolarity. Differences in the q dependence of these form factors may be interpreted as changes in the structure of the core state due, perhaps, to the blocking effect of the extra nucleon.

B. Configuration mixing model analysis

In order to predict the presence of the third octupole state in ^{89}Y at 2.86 MeV, one may augment the weak-coupling model by allowing the $2p_{1/2}$ proton to be excited to the $2d_{5/2}$ or $1g_{7/2}$ orbits.[10,11] We can thus have mixing between the $J=\frac{5}{2}$ and $J=\frac{7}{2}$ particle states and the $J=\frac{5}{2}$ and $J=\frac{7}{2}$ members of the core-excited multiplet based on the 3^- state in ^{88}Sr. This procedure introduces two levels which are assumed to be nearly degenerate at 2.86 MeV. (We previously mentioned that the state at 2.86 MeV was measured[8] to be a probable doublet.) The wave functions for the four states predicted by this model are:

$$\alpha[\phi_{1/2}\psi_v]_{5/2}-(1-\alpha^2)^{1/2}\phi_{5/2}\psi_0 \quad (2.21\ \text{MeV}),$$

$$\beta[\phi_{1/2}\psi_v]_{7/2}-(1-\beta^2)^{1/2}\phi_{7/2}\psi_0 \quad (2.52\ \text{MeV}),$$

$$\left.\begin{matrix}(1-\alpha^2)^{1/2}[\phi_{1/2}\psi_v]_{5/2}+\alpha\phi_{5/2}\psi_0 \\ (1-\beta^2)^{1/2}[\phi_{1/2}\psi_v]_{7/2}+\beta\phi_{7/2}\psi_0\end{matrix}\right\} \begin{pmatrix}2.86\ \text{MeV}\\ \text{unresolved}\end{pmatrix}.$$

$\phi_{1/2}\psi_0$ is the ^{89}Y ground-state wave function; ϕ's are single-particle-state wave functions; and ψ_0 and ψ_v are the wave functions of the ^{88}Sr ground state and 3^- state, respectively.

We determined the transition charge density parameters and strength of the 3^- level of ^{88}Sr using the Tassie model[17] in a DWBA calculation. This transition charge density was split according to the weak-coupling model to describe the expected weak-coupling octupole states in ^{89}Y. The single-particle transition charge densities were calculated as products of harmonic-oscillator wave functions. The mixed wave function transition charge densities were written into the DWBA computer code to calculate the form factors and $B(E3)\uparrow$'s of the three octupole states in ^{89}Y. The mixing parameters of the model (α and β) and the harmonic-oscillator parameter were allowed to vary to obtain the best fit to the data using an iterative nonlinear least-squares search routine. The resulting parameters are given in Table I.

APPARATUS

The high-energy electrons used in this investigation were produced by the National Bureau of Standards electron linac.[18] The energy-analyzed beam was scattered by foils of ^{88}Sr (isotopically enriched to 99.84%) and ^{89}Y mounted for transmission scattering, into a 76-cm radius of curvature, 169.8° "magic angle" spectrometer.[19] The ^{88}Sr foil was continuously kept under high vacuum and transferred into and out of the scattering chamber using a specially designed vacuum transfer cell.[20] Each of 20 semiconductor detectors[21] subtended a momentum interval ($\Delta p/p$) of 0.037% in the focal plane of the spectrometer. A triple coincidence requirement between the counts from a detector and two backup plastic scintillators was used for background rejection. The semiconductor detectors could be moved along the focal plane of the spectrometer allowing an interchange of detectors measuring the same part of a spectrum. The relative efficiencies of the detectors could then be determined by intercomparison of counting rates. The total system resolution of this experiment was 0.1% of the incident electron energy.

Absolute values of cross sections were obtained by making measurements relative to a ^{12}C target whose elastic scattering cross section (or form factor) is well known.[22,23]

Precise monitoring of total beam current was accomplished using a Faraday cup and a toroidal ferrite-core transformer periodically calibrated against the Faraday cup.[24] Data collection and partial automation of the experiment was facilitated through the use of an on-line digital computer.[25]

To determine the thickness of the ^{88}Sr, ^{89}Y, and ^{12}C targets, the latter two were weighed and their areas measured. The Sr target was cut to a premeasured area and weighed during fabrication. To check the Sr measurement, elastic form factors were calculated using the Rawitscher-Fischer (RF) phase-shift code for elastic scattering,[26] and the Fermi-charge density parameters for ^{88}Sr and ^{89}Y used by Peterson and Alster.[6] Using these form factors and the experimental elastic data at 0.55 fm^{-1}, the ^{88}Sr thickness was determined in terms of the known ^{89}Y thickness and the calculated elastic form factors. The results of these

TABLE II. Ground-state charge-density parameters.

Nucleus	c (fm)	t (fm)	rms (fm)
^{88}Sr	4.83 ± 0.01	2.18 ± 0.05	4.17 ± 0.02
^{88}Sr (work of Ref. 33)			
3-parameter Gaussian model	...	...	4.28 ± 0.02
3-parameter Fermi model	...	...	4.35 ± 0.02
^{89}Y	4.86 ± 0.01	2.38 ± 0.05	4.27 ± 0.02

thickness measurements are as follows:

^{88}Sr 4.5 mg/cm^2 (during fabrication),

4.6 mg/cm^2 (check),

^{89}Y 10.5 mg/cm^2,

^{12}C 23.2 mg/cm^2.

DATA REDUCTION

Spectra were assembled from the raw data by sorting the detector counts into constant-size energy bins after making corrections for count-rate losses, detector efficiencies, and changes in solid angle and detector momentum acceptance along the focal plane of the spectrometer. The elastic radiative tail was removed from the inelastic spectrum by fitting a function of the form

$$f(\Delta E) = A + B/\Delta E + C/(\Delta E)^2 \quad (5)$$

to the elastic tail, where ΔE is the energy difference between the elastic peak energy and the position along the radiative tail, and A, B, and C are free parameters. The peaks in the spectra were fitted using a line-shape fitting program.[20,27] The fitted line shape was constructed from considerations of radiative processes coherent with the nuclear scattering, bremsstrahlung, Landau straggling, and an assumed Gaussian shape for the electron-beam resolution function. A calculation of the error in a peak area included the statistical error and a contribution from errors correlated to the heights, widths, and positions of nearby peaks.

To extract inelastic scattering form factors, the fitted peak areas were integrated from well above the peak to three and one half linewidths below the center of the peak, and ratios of inelastic to elastic areas were calculated. Radiative corrections to elastic and inelastic peaks from the same target were essentially equal,[28] thus

$$|F_{\text{inel}}|^2 = \frac{(\text{Area) inelastic peak}}{(\text{Area) elastic peak}} |F_{\text{el}}|^2. \quad (6)$$

The elastic scattering form factors were extracted by comparison with the elastic peaks of ^{12}C. The carbon elastic form factor was calculated using the RF code. The harmonic-well parameters used in the calculation were $\alpha = 1.333$ and $a = 1.671$ fm, corresponding to a rms radius of 2.46 fm.[22] In this case the ratios of areas required radiative

TABLE III. Electron scattering form factors for ^{88}Sr.

Level	Incident energy (MeV)	Lab scattering angle (deg)	q (fm^{-1})	$\lvert F\rvert^2$	Standard deviation (%)
Ground	120.85	110.5	1.005	0.6695×10^{-2}	1.2
state	100.87	128.2	0.919	0.8558×10^{-2}	1.6
0^+	101.17	110.5	0.842	0.6633×10^{-2}	1.2
	80.86	128.2	0.737	0.1004×10^{-1}	1.7
	80.95	110.5	0.674	0.1984×10^{-1}	0.7
	67.07	128.2	0.611	0.4660×10^{-1}	0.6
	60.48	128.3	0.551	0.9065×10^{-1}	0.7
	53.46	128.3	0.487	0.1790	0.6
	45.42	128.3	0.414	0.3351	0.5
1.84 MeV	120.85	110.5	...	...	...
2^+	100.87	128.2	...	...	...
	101.17	110.5	0.834	0.2953×10^{-3}	4.7
	80.86	128.2	0.728	0.5591×10^{-3}	5.8
	80.95	110.5	0.666	0.7535×10^{-3}	3.6
	67.07	128.2	0.603	0.7610×10^{-3}	4.1
	60.48	128.3	0.543	0.9175×10^{-3}	3.1
	53.46	128.3	0.479	0.8745×10^{-3}	4.1
	45.42	128.3	0.406	0.6099×10^{-3}	4.6
2.74 MeV	120.85	110.5	0.994	0.5636×10^{-3}	4.1
3^-	100.87	128.2	0.906	0.8164×10^{-3}	5.9
	101.17	110.5	0.830	0.1086×10^{-2}	2.2
	80.86	128.2	0.724	0.1139×10^{-2}	3.2
	80.95	110.5	0.662	0.1048×10^{-2}	2.9
	67.07	128.2	0.499	0.7969×10^{-3}	3.8
	60.48	128.3	0.539	0.6788×10^{-3}	4.7
	53.46	128.3	0.475	0.4209×10^{-3}	5.9
	45.42	128.3	0.401	0.2373×10^{-3}	9.1

TABLE IV. Electron scattering form factors for ^{89}Y.

Level	Incident energy (MeV)	Lab scattering angle (deg)	q (fm^{-1})	$\|F\|^2$	Standard deviation (%)
Ground state $\frac{1}{2}^-$	120.85	110.5	1.005	0.6027×10^{-2}	0.9
	100.87	128.2	0.919	0.8147×10^{-2}	1.0
	101.17	110.5	0.842	0.6544×10^{-2}	0.8
	80.86	128.2	0.737	0.9522×10^{-2}	1.1
	80.95	110.5	0.674	0.1802×10^{-1}	0.4
	67.07	128.2	0.611	0.3496×10^{-1}	0.5
	60.48	128.3	0.551	0.8321×10^{-1}	0.5
	53.46	128.3	0.487	0.1641	0.4
	45.42	128.3	0.414	0.3258	0.3
1.51 MeV $L=2$ $\frac{3}{2}^-$	120.85	110.5	...	...	...
	100.87	128.2	...	...	...
	101.17	110.5	0.836	0.1463×10^{-4}	37.5
	80.86	128.2	0.730	0.2769×10^{-4}	39.0
	80.95	110.5	0.667	0.5404×10^{-4}	18.6
	67.07	128.2	0.604	0.6197×10^{-4}	24.1
	60.48	128.3	0.544	0.9577×10^{-4}	13.5
	53.46	128.3	0.480	0.8497×10^{-4}	12.4
	45.42	128.3	0.407	0.8282×10^{-4}	17.4
1.74 MeV $L=2$ $\frac{5}{2}^-$	120.85	110.5	...	...	...
	100.87	128.2	...	...	...
	101.17	110.5	0.835	0.2266×10^{-4}	20.8
	80.86	128.2	0.729	0.6865×10^{-4}	18.3
	80.95	110.5	0.666	0.1193×10^{-3}	8.5
	67.07	128.2	0.603	0.1301×10^{-3}	10.5
	60.48	128.3	0.543	0.1427×10^{-3}	7.2
	53.46	128.3	0.479	0.1548×10^{-3}	8.0
	45.42	128.3	0.406	0.1105×10^{-3}	11.6
2.21 MeV $L=3$ $\frac{5}{2}^+$	120.85	110.5	0.996	0.1969×10^{-3}	4.5
	100.87	128.2	0.909	0.2645×10^{-3}	7.8
	101.17	110.5	0.833	0.3397×10^{-3}	2.9
	80.86	128.2	0.727	0.3584×10^{-3}	5.1
	80.95	110.5	0.664	0.3334×10^{-3}	3.4
	67.07	128.2	0.601	0.3048×10^{-3}	5.7
	60.48	128.3	0.541	0.2478×10^{-3}	5.0
	53.46	128.3	0.477	0.1328×10^{-3}	6.5
	45.42	128.3	0.404	0.7320×10^{-4}	15.5
2.52 MeV $L=3$ $\frac{7}{2}^+$	120.85	110.5	0.995	0.1883×10^{-3}	4.8
	100.87	128.2	0.907	0.2926×10^{-3}	7.3
	101.17	110.5	0.831	0.3498×10^{-3}	2.8
	80.86	128.2	0.725	0.3711×10^{-3}	4.5
	80.95	110.5	0.663	0.3793×10^{-3}	3.0
	67.07	128.2	0.600	0.3286×10^{-3}	5.1
	60.48	128.3	0.540	0.2918×10^{-3}	2.9
	53.46	128.3	0.476	0.1593×10^{-3}	7.2
	45.42	128.3	0.402	0.7639×10^{-4}	12.9
2.86 MeV $L=3$ $(\frac{5}{2}^+, \frac{7}{2}^+)$	120.85	110.5	0.994	0.1158×10^{-3}	7.7
	100.87	128.2	0.906	0.1772×10^{-3}	9.6
	101.17	110.5	0.830	0.2310×10^{-3}	4.1
	80.86	128.2	0.724	0.2997×10^{-3}	5.4
	80.95	110.5	0.662	0.3339×10^{-3}	3.6
	67.07	128.2	0.598	0.2550×10^{-3}	5.0
	60.48	128.3	0.538	0.2357×10^{-3}	4.5
	53.46	128.3	0.474	0.1861×10^{-3}	5.2
	45.42	128.3	0.401	0.1158×10^{-3}	8.9

TABLE IV *(Continued)*

Level	Incident energy (MeV)	Lab scattering angle (deg)	q (fm^{-1})	$\|F\|^2$	Standard deviation (%)
3.1 MeV	120.85	110.5	...	...	...
$L=2$	100.87	128.2	...	...	...
$(\frac{3}{2}^-, \frac{5}{2}^-)$	101.17	110.5	0.829	0.1007×10^{-4}	38.1
	80.86	128.2	0.722	0.8593×10^{-4}	12.8
	80.95	110.5	0.661	0.1056×10^{-3}	9.0
	67.07	128.2	0.597	0.1260×10^{-3}	11.2
	60.48	128.3	0.537	0.1256×10^{-3}	8.9
	53.46	128.3	0.473	0.6261×10^{-4}	15.2
	45.42	128.3	0.400	0.1038×10^{-3}	11.1

correction because of different Z's and target thicknesses involved. Each area was integrated to five linewidths below the center of the peak and corrected for Schwinger,[29] bremsstrahlung,[30] and ionization effects.[31] Thus

$$|F|^2 = \frac{A'}{A'_c} |F_c|^2 \left(\frac{Z_c}{Z}\right)^2 \frac{t_c/A_c}{t/A}, \tag{7}$$

where A' and A'_c are the elastic peak areas corrected for radiative effects, and t, A and t_c, A_c are the thickness and mass number of the target and carbon target, respectively.

RESULTS

The ^{88}Sr and ^{89}Y elastic scattering form factors were fitted using the RF code. The program was used to calculate σ/σ_M corresponding to each experimental point. A χ^2 was calculated to measure the quality of fit of the calculations to the experimental points. Target thickness was used as a parameter in addition to the two Fermi-model parameters in order to remove uncertainties in the fit due to a possible error in the measured target thickness. Magnetic elastic scattering from ^{89}Y was assumed to be negligible. The best-fit values of the parameters were determined using an iterative nonlinear least-squares search procedure. This procedure also established the errors associated with each fitted parameter from the error matrix[32] derived in the search. We determined that a 3% standard deviation must be assigned to

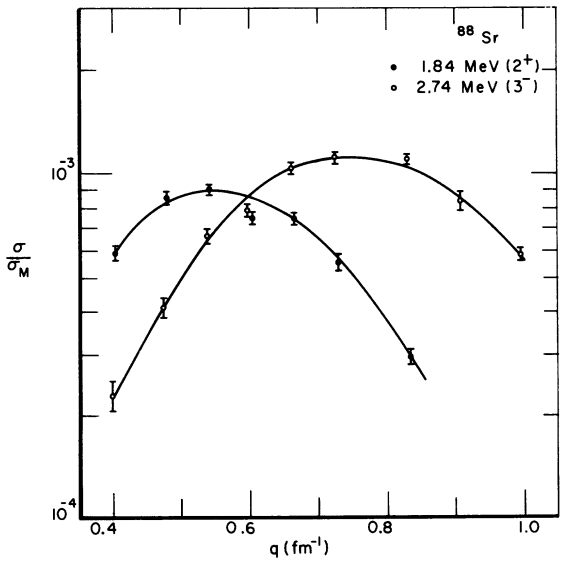

FIG. 5. Tassie-model fits to ^{88}Sr 2^+ and 3^- form factors.

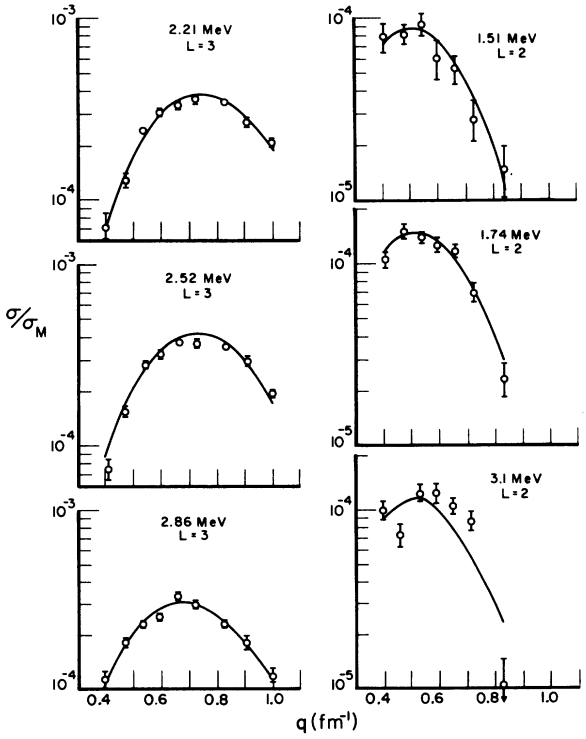

FIG. 6. Tassie-model fits to ^{89}Y form factors.

each measured cross section in order to produce a χ^2 of one per degree of freedom. The results are shown in Figs. 3 and 4 and Table II along with a comparison with the recent Stanford determination[33] of the rms radius of ^{88}Sr.

We have extracted form factors for the following inelastic levels:

^{88}Sr 1.84 MeV, 2^+; 2.74 MeV, 3^-

^{89}Y 1.51 MeV, $\frac{3}{2}^-$; 1.74 MeV, $\frac{5}{2}^-$;
2.21 MeV, $\frac{5}{2}^+$; 2.52 MeV, $\frac{7}{2}^+$;
2.86 MeV, $(\frac{5}{2}^+, \frac{7}{2}^+)$; 3.1 MeV, $(\frac{3}{2}^-, \frac{5}{2}^-)$.

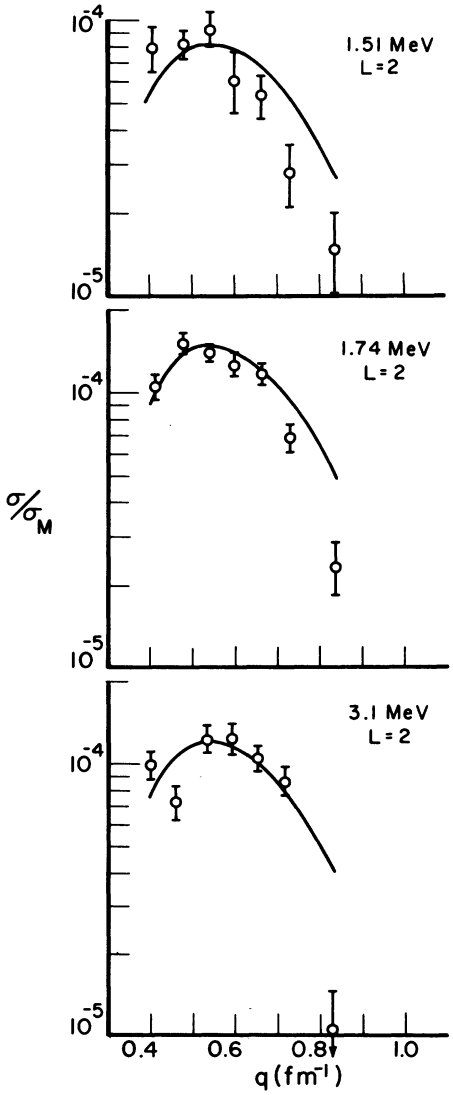

FIG. 7. Form factors for quadrupole transitions in ^{89}Y compared with the q dependence of the state at 1.84 MeV in ^{88}Sr. The solid curves have the same shape as the Tassie-model 2^+ level fit shown in Fig. 5.

The inelastic form factor uncertainties shown in Tables III and IV and Figs. 5–8 are standard deviations due primarily to counting statistics.

Reduced transition probabilities $B(EL)\uparrow$ were determined using the DWBA code. The transition charge density ρ_{tr} was given by the Tassie model,[17] i.e.,

$$\rho_{tr} = K r^{L-1} \frac{\partial \rho}{\partial r}, \tag{8}$$

where ρ is the Fermi-charge distribution. The Fermi-model parameters (c, z) were allowed to vary in the calculation of ρ_{tr} to produce the best fit to an inelastic form factor.

The octupole triplet in ^{89}Y was also fitted using the configuration mixing model discussed previously. In this case the resultant $B(EL)\uparrow$'s for these levels are a prediction based on the mixed model employed for the transition charge density. These predictions may be compared with the Tassie-model fits to the same levels which determined the experimentally measured $B(EL)\uparrow$'s. It should be kept in mind that the experimentally determined $B(EL)\uparrow$'s are somewhat model dependent. Specifically the Tassie-model fit to the 2.86-MeV level in ^{89}Y required a large change in the transition charge density parameters compared to the other members of the octupole triplet. This effectively changed the model used and introduced an uncertainty in

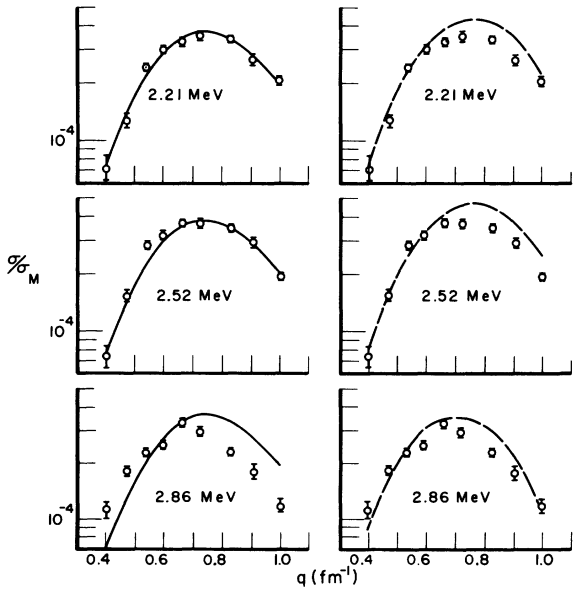

FIG. 8. Form factors of the octupole triplet in ^{89}Y compared to the q dependence of the ^{88}Sr 3^- transition and to the predictions of the mixed model. The solid curves have the same shape as the Tassie-model 3^- level fit shown in Fig. 5. The dashed curves are the predictions of the configuration mixing model described in the text, using the parameters given in Table I.

TABLE V. Reduced transition probabilities [$B(EL)\uparrow$].

Nucleus	Level	$B(EL)\uparrow$ (Tassie model) (e^2 fm^{2L})	$B(EL)\uparrow$ (Tassie model) Weisskopf units	Prediction of mixed model $B(EL)\uparrow$ for ^{89}Y 3^- transitions (e^2 fm^6)	Prediction of mixed model $B(EL)\uparrow$ for ^{89}Y 3^- transitions Weisskopf units
^{88}Sr	2^+, 1.84 MeV	822.4 ± 23.8	7.0 ± 0.2		
	3^-, 2.74 MeV	62 034 ± 4015	19.3 ± 1.2		
^{89}Y	$\frac{3}{2}^-$, $L=2$ 1.51 MeV	130.7 ± 17.57	1.1 ± 0.1		
	$\frac{5}{2}^-$, $L=2$ 1.74 MeV	196.8 ± 13.89	1.7 ± 0.1		
	$\frac{5}{2}^+$, $L=3$ 2.21 MeV	25 777 ± 2251	7.8 ± 0.7	24 836	7.5
	$\frac{7}{2}^+$, $L=3$ 2.52 MeV	36 603 ± 2818	11.1 ± 0.9	25 764	7.8
	$(\frac{5}{2}^+, \frac{7}{2}^+)$, $L=3$ 2.86 MeV	50 536 ± 5000	15.3 ± 1.5	30 160	9.2
	$(\frac{3}{2}^-, \frac{5}{2}^-)$, $L=2$ 3.1 MeV	144.6 ± 11.66	1.2 ± 0.1		

the extracted value of $B(E3)\uparrow$ for this level, which is not reflected in the stated uncertainty.

All inelastic form-factor fits were carried out using the iterative nonlinear least-squares search procedure. The experimental form factors were first normalized to a single incident energy (120.85 MeV) and treated as though q had been varied by changing the scattering angle rather than the energy, in order to decrease the amount of needed computer time. The sensitivity of this technique to the transition charge parameters used was removed by iterating the fitting and renormalizing procedure. The $B(EL)\uparrow$'s are given in Table V. The ρ_{tr} parameters are given in Table VI.

CONCLUSIONS

A. Elastic scattering

The Fermi-charge density parameters obtained in the fits to the elastic scattering data reveal that the increase in the half-density radius (c) between ^{88}Sr and ^{89}Y follows an $A^{1/3}$ law. The increase in the skin thickness parameter (z) between ^{88}Sr and ^{89}Y is consistent with the presence of a loosely bound proton in ^{89}Y.

B. Inelastic scattering

The extracted reduced transition probabilities reveal the extent to which model dependence may influence the value of $B(EL)\uparrow$ in this momentum transfer range. A comparison of the $B(E3)\uparrow$'s obtained for the 2.86-MeV level using the Tassie model and the configuration mixing model yield values for $B(E3)\uparrow$ for this level differing by ~50%. Even though the configuration mixing model result is a prediction rather than a fit, adjustment of the predicted form factor to more closely fit the experimentally measured form factor only increases the difference between these two results.

A comparison of the Tassie-model transition strengths of the first two members of the octupole triplet to a prediction of the weak-coupling model reveals good agreement in that:

(1) The sum of the strengths of the two ^{89}Y states nearly equals the strength of the ^{88}Sr core state (see Table V).

(2) The ratio of the strengths of the members of the multiplet are approximately $(2j_2+1)/(2j_1+1)$

TABLE VI. Ratios of half-density radius and skin-thickness parameters used in ρ_{tr} to ground-state values; radv and skv, respectively, determined by Tassie model fits to inelastic form factors.

Nucleus	Level	radv	skv
^{88}Sr	2^+ 1.84 MeV	0.95 ± 0.01	1.0
	3^- 2.74 MeV	0.97 ± 0.04	0.88 ± 0.13
^{89}Y	$\frac{3}{2}^-$ 1.51 MeV	1.05 ± 0.04	1.0
	$\frac{5}{2}^-$ 1.74 MeV	1.01 ± 0.02	1.0
	$\frac{5}{2}^+$ 2.21 MeV	0.84 ± 0.05	1.10 ± 0.10
	$\frac{7}{2}^+$ 2.52 MeV	0.80 ± 0.05	1.25 ± 0.08
	$(\frac{5}{2}^+, \frac{7}{2}^+)$ 2.86 MeV	0.69 ± 0.07	1.54 ± 0.08
	$(\frac{3}{2}^-, \frac{5}{2}^-)$ 3.1 MeV	1.0 ± 0.02	1.0

$= 4/3$ (see Table V) where j_1 and j_2 are the spins of the first and second members of the octupole triplet in ^{89}Y.

The q dependence of these two states is also the same as that of the 3^- state in ^{88}Sr, unlike the q dependence of the third member of the triplet at 2.86 MeV which is different than the other 3^- transitions.

The prediction of the presence of the third octupole transition in ^{89}Y is accomplished using the configuration mixing model. The calculation produces the strengths and shapes of the octupole triplet based on the measured strength of the ^{88}Sr 3^- level, and two single-particle transitions described by simple harmonic-oscillator wave functions. The resulting mixed wave functions also maintain the collective character of the first two members of the octupole triplet, thus leaving the essentially weak-coupled nature of these states intact. No effective charge was used in this calculation.

A comparison of the quadrupole doublet at 1.51 and 1.74 MeV in ^{89}Y to the weak-coupling-model predictions yields the following results. The ratios of the strengths of the $\frac{5}{2}^-$ to the $\frac{3}{2}^-$ levels are in good agreement with the weak-coupling prediction of 1.5. However, the summed strengths of the two levels is only ~40% of the 2^+ level strength in ^{88}Sr. We also note that the form factors of the doublet fall, with increasing q, more rapidly than the 2^+ form factor in ^{88}Sr, leading to the conclusion that the core state is not being excited in the same sense as in ^{88}Sr. We also noted previously that these 2^+ transitions in both nuclei are excited by single-proton pickup reactions. Thus, the 2^+ state in ^{88}Sr possesses a large single-particle component, and is partially blocked by the presence of the $2p_{1/2}$ proton in ^{89}Y.

It is clear from the various experiments exciting the 2^+ state in ^{88}Sr that the state is somewhat collective, but also has large single-hole components. Interestingly, these are the same holes used to describe the 2^+ doublet in ^{89}Y. Thus the core, although certainly modified by blocking, is still being excited in ^{89}Y. In addition the correct spins and parities, number of states, excitation energies, and ratios of strengths seem to reinforce a weak-coupling description. Perhaps what we observe is a region where weak-coupling states have become nearly single-hole states due to the low collectivity of the core. In other words, we are somewhere between the two extreme models in describing the quadrupole doublet in ^{89}Y.

The peak at 3.1 MeV in ^{89}Y has been shown to be three unresolved levels in the high-resolution proton inelastic scattering study mentioned previously. We thus simply report the measurements of the apparent 2^+ over-all form factor and $B(E2)\uparrow$ for this peak.

[1] A. de-Shalit, Phys. Rev. 122, 1530 (1961); A. Arima and I. Hamamoto, Annu. Rev. Nucl. Sci. 21, 55 (1971).
[2] S. M. Shafroth, P. N. Trehan, and D. M. Van Patter, Phys. Rev. 129, 704 (1963).
[3] J. Alster, D. C. Shreve, and R. J. Peterson, Phys. Rev. 144, 999 (1966).
[4] M. M. Stautberg, J. J. Kraushaar, and B. W. Ridley, Phys. Rev. 157, 977 (1967).
[5] J. Picard and G. Bassani, Nucl. Phys. A131, 636 (1969).
[6] G. A. Peterson and Jonas Alster, Phys. Rev. 166, 1136 (1968).
[7] C. D. Kavaloski, J. S. Lilley, D. C. Shreve, and Nelson Stein, Phys. Rev. 161, 1107 (1967).
[8] P. F. Hinrichsen, S. M. Shafroth, and D. M. Van Patter, Phys. Rev. 172, 1134 (1968).
[9] N. F. Mott, Proc. R. Soc. Lond. A124, 425 (1929).
[10] F. H. Lewis, Jr., B. F. Gibson, and M. S. Weiss, Bull. Am. Phys. Soc. 13, 719 (1968).
[11] F. H. Lewis, Jr., B. F. Gibson, and M. S. Weiss, to be published.
[12] T. deForest and J. D. Walecka, Adv. Phys. 15, 1 (1966).
[13] L. I. Schiff, Phys. Rev. 87, 750 (1954).
[14] J. D. Walecka, Phys. Rev. 126, 653 (1962).
[15] E. R. Cosman and D. C. Slater, Phys. Rev. 172, 1126 (1968).
[16] J. C. Hafele, Phys. Rev. 159, 996 (1967).
[17] L. J. Tassie, Aust. J. Phys. 9, 407 (1956).
[18] J. E. Leiss, Los Alamos Scientific Laboratory Report No. LA-3609, 1966 (unpublished), p. 20.
[19] S. Penner and J. W. Lightbody, Jr., in *Proceedings of the International Symposium on Magnet Technology, Stanford, California, 1965*, edited by H. Brechna and H. S. Gordon (Stanford Linear Accelerator, 1965), p. 154. Available from Clearinghouse for Federal Scientific and Technical Information, Springfield, Va.
[20] S. P. Fivozinsky, Ph.D. thesis, University of Connecticut, 1971 (unpublished).
[21] J. W. Lightbody, Jr., and S. Penner, IEEE Trans. Nucl. Sci. NS-15, 419 (1968).
[22] J. A. Jansen, R. Th. Peerdeman, and C. DeVries, Nucl. Phys. A188, 337 (1972).
[23] I. Sick and J. S. McCarthy, Nucl. Phys. A150, 631 (1970).
[24] J. S. Pruitt, Nucl. Instrum. Methods 92, 285 (1971).
[25] J. Broberg, IEEE Trans. Nucl. Sci. NS-13, 192 (1966).
[26] G. H. Rawitscher and C. R. Fischer, Phys. Rev. 122, 1330 (1961); C. R. Fischer and G. H. Rawitscher, Phys. Rev. 135, B377 (1964).
[27] J. C. Bergstrom, U.S. Atomic Energy Commission Report No. TID-24667, 1967 (unpublished), MIT Summer Study, 1967.
[28] L. Maximon, Ref. 27.
[29] J. Schwinger, Phys. Rev. 75, 898 (1949).
[30] Hoan Nguyen Ngoc and Jean P. Perez-Y-Jorba, Phys. Rev. 136, B1030 (1964).
[31] L. Landau, J. Phys. USSR 8, 201 (1944).
[32] P. Bevington, *Data Reduction and Error Analysis for the Physical Sciences* (McGraw-Hill, New York, 1969).
[33] J. Alster, B. Gibson, J. McCarthy, M. Weiss, and R. Wright, Phys. Rev. C 7, 1089 (1973).